Structure, Stability, and Thermodynamics of Lamellar DNA-Lipid Complexes

Daniel Harries,* Sylvio May,* William M. Gelbart,† and Avinoam Ben-Shaul*

*Department of Physical Chemistry and the Fritz Haber Research Center, The Hebrew University of Jerusalem, Jerusalem 91904, Israel, and †Department of Chemistry and Biochemistry, University of California Los Angeles, Los Angeles, California 90095 USA

ABSTRACT We develop a statistical thermodynamic model for the phase evolution of DNA-cationic lipid complexes in aqueous solution, as a function of the ratios of charged to neutral lipid and charged lipid to DNA. The complexes consist of parallel strands of DNA intercalated in the water layers of lamellar stacks of mixed lipid bilayers, as determined by recent synchrotron x-ray measurements. Elastic deformations of the DNA and the lipid bilayers are neglected, but DNA-induced spatial inhomogeneities in the bilayer charge densities are included. The relevant nonlinear Poisson-Boltzmann equation is solved numerically, including self-consistent treatment of the boundary conditions at the polarized membrane surfaces. For a wide range of lipid compositions, the phase evolution is characterized by three regions of lipid to DNA charge ratio, ρ: 1) for low ρ, the complexes coexist with excess DNA, and the DNA-DNA spacing in the complex, d, is constant; 2) for intermediate ρ, including the isoelectric point $\rho = 1$, all of the lipid and DNA in solution is incorporated into the complex, whose inter-DNA distance d increases linearly with ρ; and 3) for high ρ, the complexes coexist with excess liposomes (whose lipid composition is different from that in the complex), and their spacing d is nearly, but not completely, independent of ρ. These results can be understood in terms of a simple charging model that reflects the competition between counterion entropy and inter-DNA ($\rho < 1$) and interbilayer ($\rho > 1$) repulsions. Finally, our approach and conclusions are compared with theoretical work by others, and with relevant experiments.

INTRODUCTION

It is difficult to imagine a biological structure or process in which electrostatics do not play a significant role. This is because of the charge carried by virtually all proteins, polynucleotides (e.g., DNA), and cell membranes. Accordingly, it is not surprising that attempts to understand the interaction of specific proteins with DNA, and with cell membranes, have inspired researchers to focus a great deal of theoretical effort on practical ways of determining the distribution of mobile counterions and their consequent screening effects in aqueous solution (Honig and Nicholls, 1995). Similarly, in recent discussions of liposomal vectors for gene delivery, i.e., targeting of extracellular DNA into cell nuclei, fundamental electrostatic issues arise immediately because of the strong interactions between the DNA and cationic lipids used to complex it (Felgner et al., 1987, 1996; Felgner and Ringold, 1989; Gershon et al., 1993; Gustafsson et al., 1995; Lasic et al., 1997; Zuidam and Barenholz, 1997; Hui et al., 1996; Mok and Cullis, 1997).

A most compelling example is provided by the studies of Rädler et al. (Rädler et al., 1997; Salditt et al., 1997), who report the existence of highly novel DNA-cationic liposome complexes, as determined by high-resolution synchrotron x-ray diffraction and optical microscopy. In particular, the lipoplex is shown to consist of multilayer lamellar stacks of charged bilayer, each consisting of a mixture of charged DOTAP (dioleoyltrimethylammonium-propane) and neutral DOPC (dioleoylphosphatidylcholine) lipid, with the parallel DNA strands intercalated between.

Quite different morphologies are expected to arise for other choices of neutral ("helper") lipid; in the case of DOPE (dioleoylphosphatidylethanolamine), for example, inverted hexagonal ("honeycomb") organization of the lipid, with single strands of DNA in aqueous solution regions, is implicated (Felgner et al., 1987; Tarahovsky et al., 1996). "Spaghetti" structures have also been reported, in which each DNA strand is coated by a cylindrical bilayer of the cationic/neutral lipid mixture (Sternberg et al., 1994; Sternberg, 1996). Both of these honeycomb and spaghetti-like structures have recently been investigated theoretically (May and Ben-Shaul, 1997; Dan, 1998).

In the present paper we treat in detail the electrostatics and self-assembly characteristics of the multibilayer lamellar stacks of intercalated DNA, structures that we shall refer to henceforth as L_α^c complexes (see Fig. 1). We address them within the general context of the statistical thermodynamics of aqueous solutions of DNA and mixtures of neutral and cationic lipids (see Theory). Mobile counterions are described by the nonlinear Poisson-Boltzmann (PB) equation, which is solved numerically. Although we neglect elastic deformations of the DNA strands and bilayers, we do allow for the possibility of spatial inhomogeneities in the membrane surface charge density, in response to interactions with the anionic DNA. This effect turns out to be significant, and reflects the "extra" degree of freedom associated with cationic lipids in *mixed, fluid* bilayers. In solving the PB equation, then, we need to treat the (Gauss law) boundary conditions at the membrane surface in a fully

Received 29 January 1998 and in final form 6 April 1998.

Address reprint requests to Dr. Avinoam Ben-Shaul, Department of Physical Chemistry, The Fritz Haber Research Center, Jerusalem 91904, Israel. Tel.: 972-2-6585271; Fax: 972-2-6513742; E-mail: abs@fh.huji.ac.il.

0006-3495/98/07/159/15 $2.00

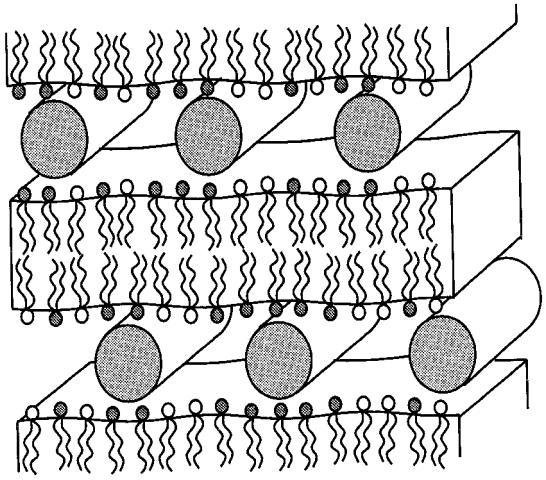

FIGURE 1 Schematic illustration of the lamellar (L_α^c) lipid-DNA complex.

self-consistent way, because the charge density there varies along the direction normal to the DNA strands, and does so in a way that depends on the distribution of counterions (electrostatic potential), which in turn depends on the charge at the surface. We do this in the Results section for a wide range of DNA-DNA spacings, overall lipid composition, and added salt concentrations. We then determine the phase evolution of the system by calculating free energies and solving the equations that express equilibrium between the L_α^c complex and, alternately, excess DNA and excess lipid. In this way we establish how DNA-DNA spacings d vary with the ratio ρ of charged lipid to DNA, for each of several different lipid compositions (ratio of neutral to cationic lipid). In agreement with experiment, we find that for a lipid mixture of given composition, the spacings are constant throughout the low ρ range, where the complex coexists with excess DNA. In the high ρ range, where the complex coexists with excess lipid, the spacings are nearly constant as well. Throughout the "single-phase" region, however, where all of the DNA and lipids are accommodated by the complex, the DNA-DNA spacings increase linearly with ρ, as implied by material conservation. This region is found to include the special ("isoelectric") point at which the total charges carried by DNA and lipid are equal. Moreover, at the isoelectric point the free energy of the complex is minimal.

All of the above results can be qualitatively accounted for by a simple model described in the Discussion, in which the electrostatic effects enter only via the "excess charge" that measures the extent of deviation from the isoelectric point. In this way one can understand the constancy of DNA-DNA spacings at low and high ρ, i.e., at large deviations from the isoelectric point, directly in terms of the mutual repulsions between like-charged DNA strands or lipid bilayer surfaces, respectively. We include in the final section a brief account of the theory of the L_α^c complex presented independently by Bruinsma (1998), who interprets the observed structural evolution (d versus ρ) via approximate analytical solution of the nonlinear PB theory. His analysis of the free energy (which is restricted to low cationic lipid contents) is based on a physical picture that is quite similar to ours; his conclusions regarding the phase evolution of the system are somewhat different. We also discuss there the quite different approach suggested by Dan (1996, 1997), who, in contrast, ascribes the preferred d spacing at low ρ to a competition between short-range electrostatic repulsions and longer-ranged DNA-DNA attractions mediated by the elastic deformation of the bilayer membranes.

THEORY

In this section we outline our model for calculating the free energy of the L_α^c complex, and derive the thermodynamic relationships dictating the complex structure and phase behavior in lipid-DNA solutions, as a function of the overall lipid-to-DNA ratio and the cationic/neutral lipid composition.

Model

Ignoring edge effects, we shall treat the complex as an infinite periodic lamellar array consisting of alternating lipid bilayers and DNA monolayers, as schematically illustrated in Fig. 1. The DNA strands are assumed to be infinite, parallel, and equidistant rigid rods, thus forming a one-dimensional (1D) lattice. As noted in the previous section, the existence of a well-defined interaxis distance d (which depends on lipid composition and lipid-to-DNA ratio) has been unequivocally confirmed by x-ray diffraction studies (Rädler et al., 1997). Theoretical support for this finding will be given in the following sections. The naked DNA strands in solution will be treated as infinite cylindrical rods, and the liposomal membranes as perfectly planar infinite bilayers.

In modeling the DNA strands as infinite rods, we ignore the effects associated with their flexibility, in particular curvature fluctuations and undulation forces (Podgornik et al., 1989, 1994; Strey et al., 1997). This approximation is justified in view of the fact that the DNA persistence length ($\xi \approx 500$ Å) is significantly larger than all of the other relevant length scales in the L_α^c complex, namely, the DNA radius $R \approx 10$ Å, the interaxial distance $d \approx 20$–70 Å, the thickness of the interbilayer water gap $h \approx 25$ Å, the bilayer thickness $w \approx 30$ Å, and the average linear dimension of a lipid headgroup $a^{1/2}$, where $a \approx 70$ Å^2 is the average cross-sectional area per lipid molecule in the membrane. It should be noted that any curvature fluctuation of an individual DNA strand within the monolayer implies a change in d extending over a distance of order ξ. From the calculations presented in the next section, it will become apparent that such changes involve an electrostatic free energy penalty of several k_BT's, indicating that curvature and interaxis fluctuations in the complex are rather small (k_B is Boltzmann's constant and T is the absolute temperature).

Another assumption that will be made in this work is that the lipid bilayers are perfectly planar, and their thickness, w,

is constant and independent of their lipid composition. In general, one cannot exclude the possibility of membrane curvature modulations induced by the DNA lattice (as schematically illustrated in Fig. 1). For lipid bilayers of high bending rigidity (Helfrich, 1973), these modulations are expected to play a minor role in determining the complex stability. On the other hand, when "soft" bilayers are involved in complex formation, these curvature modulations may become increasingly important, possibly leading to structural phase transformations involving, say, the inverted hexagonal/honeycomb states mentioned in the Introduction. The assumption of constant w is justified for bilayers whose cationic and neutral lipid components are of similar chain length. This is the case for the neutral lipids DOPC and DOPE, as well as the cationic lipid DOTAP, mixtures of which are known to form lamellar complexes with DNA (Rädler et al., 1997). The extension of our model to cases where w varies with the lipid composition is, in principle, straightforward.

The negative charges on the DNA surface are densely spaced; the average spacing between these charges along the axis of B-DNA is $l = 1.7$ Å. We shall assume that these charges form a continuous and uniform charge distribution over the DNA surface, which will be regarded as a perfect cylindrical envelope. This approximation is supported by numerical studies revealing that the electrostatic potential around the DNA surface is not different from that produced by a continuous charge distribution, except for a narrow region in its immediate vicinity (Wagner et al., 1997). In all of our calculations, we shall use $R = 10$ Å for the radius of this cylinder, implying a uniform charge density $\sigma^- = e/2\pi Rl \approx 0.15\ \mathrm{Cm}^{-2}$, corresponding, approximately, to one elementary charge, e, per 110 Å^2.

We shall also assume that the cationic and neutral lipids constituting the membrane are ideally mixed. In the free bilayer this implies, on average, a uniform and continuous charge distribution. The charge density is $\sigma^+ = e\phi/a$, where ϕ is the mole fraction of the cationic lipids and a is the average area per lipid headgroup. On the other hand, in the bilayers of the complex we shall allow for spatial modulations of the cationic charges, while assuming that ideal mixing applies *locally*. In all calculations we shall use $a = 70$ Å^2 (implying $\sigma^- = \sigma^+$ when $\phi \approx 0.65$) for both lipid components, in both the free and the complexed bilayer.

Finally, the naked DNA, the free lipid bilayer, and the lipid-DNA complex will be treated as macroscopic phases, i.e., we ignore the free energy contributions associated with their overall translational and rotational degrees of freedom. These free energies are on the order of $1k_BT$ per particle, much less than their "internal" (electrostatic and mixing) free energies.

Free energies

We define a unit cell of a complex as a rectangular box of dimensions $d \times b \times s$, where d is the distance, along the x axis, between two neighboring DNA strands; $b = h + w$ is the distance between two bilayer midplanes along the y axis; and s is the "depth" of the unit cell along the z (the DNA axis) direction. Because the complex is translationally invariant along the z axis, the calculation of the complex free energy is a 2D problem, and the choice of s is arbitrary (Fig. 2). Our numerical results will be reported for $s = 1$ Å. For the numerical evaluation of the complex free energy, it is convenient to consider only one-quarter of a unit cell, as shown in Fig. 2.

Formation free energy

Let $f_C = f_C(\phi, d, h)$ denote the free energy of one unit cell of the complex, where $\phi = \phi_C$ is the average mole fraction of the cationic lipid in the complex. Alternatively, we may interpret f_C as the free energy of a DNA strand (of length s), when incorporated in a complex characterized by ϕ_C, d, h plus the free energy of a complexed bilayer segment containing $n = 2s \times d/a$ lipid molecules. In the limit $d \to \infty$, $h \to \infty$, the complex disintegrates into well-separated DNA and lipid bilayer. Thus $f_C(\phi, d \to \infty, h \to \infty) = f_D + f_B(\phi) = f_D + d\tilde{f}_B(\phi)$. Here f_D is the free energy of a naked DNA rod of length s, and $f_B(\phi)$ is the free energy of a bare bilayer segment of area $s \times d$; $\tilde{f}_B(\phi) = f_B(\phi)/d$ may be interpreted as the free energy per unit length of a bilayer strip of width s. ($f_B/n = (a/2s)\tilde{f}_B$ is the free energy per lipid molecule in the bilayer.) Conversely, the difference

$$\Delta f_C(\phi, d, h) = f_C(\phi, d, h) - f_D - d\tilde{f}_B(\phi) \qquad (1)$$

may be regarded as the free energy change associated with complex formation from its separate, DNA and lipid bilayer, components. A complex characterized by ϕ, d, and h is thermodynamically stable only if $\Delta f_C < 0$. We now turn

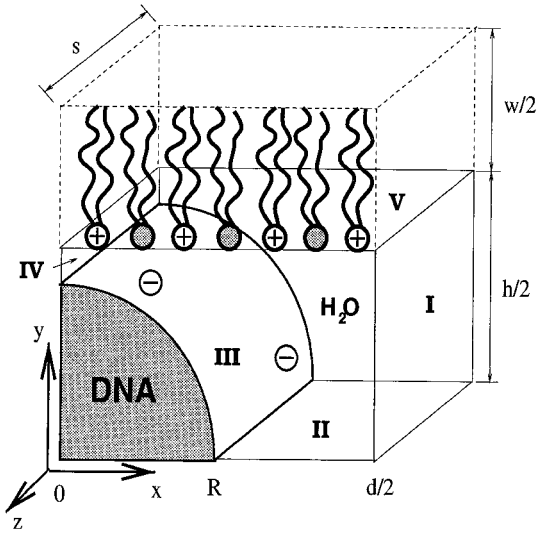

FIGURE 2 Schematic representation of one-quarter of the complex's unit cell. The Poisson-Boltzmann equation is solved in the aqueous interior subject to boundary conditions appropriate for surfaces I–V (see text).

to a more detailed discussion of the terms appearing on the right-hand side of Eq. 1.

Complex

As we do not allow for curvature or thickness modulations of the lipid layers, f_C involves only two contributions: the electrostatic (charging) free energy of the complex and the (in-plane) lipid mixing entropy. Although, locally, the two lipid components are ideally mixed, the presence of the negatively charged DNA grid can induce a spatial modulation (or "polarization") of the cationic lipid charges (along the x axis), to minimize the electrostatic energy of the system. However, this tendency is opposed by the lipid *"demixing" entropy* penalty associated with any deviation from a uniform distribution. The extent of lipid demixing (charge modulation) is governed by a delicate interplay between these two opposing tendencies. That is, the electrostatic and lipid mixing contributions to the complex free energy are strongly coupled. Thus the lipid composition profile $\eta(x)$, the electrostatic potential in the complex interior $\varphi(x, y)$, and the actual value of the complex's free energy, $f_C(\phi, d, h)$, must be determined by minimizing the total free energy functional, which includes both the mixing and electrostatic terms, namely,

$$f_C = \left(\frac{k_B T}{e}\right)^2 \int_v \frac{\epsilon}{2}(\nabla\psi)^2 dv + k_B T \int_v \left[n_+ \ln\frac{n_+}{n_0} + n_- \ln\frac{n_-}{n_0} - (n_+ + n_- - 2n_0)\right] dv + \frac{k_B T}{a}\int_{S_v} [\eta \ln \eta + (1-\eta)\ln(1-\eta)] dS. \quad (2)$$

The first term on the right-hand side of this equation is the electrostatic energy; $\psi = e\varphi/k_B T$ is the scaled (dimensionless) electrostatic potential; and $\epsilon = \epsilon_0\epsilon_r$, where ϵ_r is the dielectric constant of the solution and ϵ_0 is the permittivity of vacuum (Verwey and Overbeek, 1948). The integration is over the volume of the unit cell. We use $\epsilon_r = 78$ for the aqueous regions, and assume $\epsilon = 0$ in the interior of the DNA and the lipid membrane. The second term accounts for the translational ("mixing") entropy of the mobile ions in the complex interior, relative to their entropy in the bulk solution, with $n_+ = n_- = n_0$, $n_\pm = n_\pm(x, y)$ denoting the local concentrations of mobile ions in the complex. (We assume a 1:1 electrolyte solution.) The last term accounts for the mixing entropy of the charged and neutral lipids in the membrane plane. The integration is over the membrane surface (surface V in Fig. 2). Locally, i.e., at any x, the lipids are assumed to be ideally mixed, with $\eta = \eta(x)$ denoting the local mole fraction of the charged lipid. (Recall that the average area per lipid in the membrane is assumed to be independent of the lipid composition.) The local lipid composition must satisfy the conservation constraint

$$\phi = \frac{\int_{S_v} \eta\, dS}{\int_{S_v} dS}, \quad (3)$$

where ϕ is the mean mole fraction of the charged lipid in the complex.

Functional minimization of f_C with respect to n_+, n_- and η, subject to the conservation constraint (Eq. 3), yields the following results. For the mobile ion distributions, one finds the usual Boltzmann distributions, $n_\pm = n_0 \exp(\mp\psi)$, which upon substitution into Poisson's equation, yield the PB equation,

$$\nabla^2\psi = \kappa^2 \sinh\psi, \quad (4)$$

where $\kappa^{-1} = (\epsilon_0\epsilon_r k_B T/2n_0 e^2)^{1/2} \equiv l_D$ is the Debye length.

For $\sigma^+(x) = e\eta(x)/a$, the local charge density on the membrane, we obtain

$$\eta = \frac{e^{-(\psi+\lambda)}}{(1-\phi)/\phi + e^{-(\psi+\lambda)}} = -\alpha\nabla\psi\cdot\hat{\mathbf{n}}, \quad (5)$$

where $\alpha = a\epsilon k_B T/e^2$, λ is the Lagrange multiplier conjugate to the charge conservation constraint (Eq. 3), and $\hat{\mathbf{n}}$ is the unit vector normal to the boundary (pointing into the dielectric medium). The second equality in Eq. 5 is Gauss' equation, relating the local surface charge density at x to the electrostatic potential at the membrane surface. This equation represents one of the boundary conditions (boundary V in Fig. 2) on the electrostatic potential and must be solved simultaneously, and self-consistently, with the PB equation (Eq. 4). Note that for our model of the L_α^c complex, both equations are 2D.

The other boundary conditions, pertaining to domain boundaries I–IV in Fig. 2, are less intricate. At the DNA surface (domain boundary III), the boundary condition is that of constant charge density, $-\nabla\psi\cdot\hat{\mathbf{n}} = e\sigma^-/\epsilon_0\epsilon_r k_B T$. For domain boundaries I, II and IV we have, by symmetry, $\partial\psi/\partial x|_I = 0$, $\partial\psi/\partial y|_{II} = 0$, $\partial\psi/\partial x|_{IV} = 0$. The numerical procedure for solving the PB equation (Carnie et al., 1994; Stankovich and Carnie, 1996; Houstis et al., 1985) and for evaluating λ, ψ and the free energy of the complex is outlined in the Appendix.

Bare bilayer, naked DNA

The free energy of the bare bilayer is a sum of mixing and electrostatic contributions, $f_B = f_B^m + f_B^e$, both depending on the lipid composition ϕ. (By symmetry, at equilibrium, the bilayer is planar and the lipid compositions in its two monolayers are identical.) The mixing entropy contribution (per unit length of a bilayer strip of width s) is

$$\tilde{f}_B^m = (2s/a)k_B T[\phi \ln\phi + (1-\phi)\ln(1-\phi)]. \quad (6)$$

For $\tilde{f}_B^e$ we can use a closed-form expression for the electrostatic free energy of a charged planar surface (Lekkerkerker,

1989):

$$\tilde{f}_{\mathrm{B}}^{\mathrm{e}} = 2(2s/a)k_{\mathrm{B}}T\phi\left[\frac{1-q}{p} + \ln(p+q)\right], \qquad (7)$$

with $p = 2\phi l_{\mathrm{B}}\,\pi/(\kappa a)$ and $q = \sqrt{p^2+1}$; $l_{\mathrm{B}} \equiv e^2/(4\pi\epsilon k_{\mathrm{B}}T)$ is the Bjerrum length (in water at room temperature $l_{\mathrm{B}} = 7.14$ Å). Note that, with the identification of $l_{\mathrm{C}} \equiv e/2\pi\sigma l_{\mathrm{B}}$ as the Gouy-Chapman length ($\sigma = e\phi/a$), and $l_{\mathrm{D}} \equiv \kappa^{-1}$ as the Debye length, p is recognized to be the ratio of fundamental lengths, $p = l_{\mathrm{D}}/l_{\mathrm{C}}$.

In Fig. 3 we show the bilayer free energy per molecule, $f_{\mathrm{B}}/n = (f_{\mathrm{B}}^{\mathrm{m}} + f_{\mathrm{B}}^{\mathrm{e}})/n$, as a function of the lipid composition, ϕ_{B}, for two values of the Debye length, $l_{\mathrm{D}} = 50$ Å and 10 Å. It should be noted that the electrostatic (charging) energy is a monotonically increasing function of ϕ_{B}; the shallow minimum of f_{B} at small ϕ_{B} is due to the lipid entropy contribution, $f_{\mathrm{B}}^{\mathrm{m}}$ (whose minimum is at $\phi_{\mathrm{B}} = 1/2$). Also shown in this figure is (the constant) energy for charging a naked DNA of length $a/2\pi R$, corresponding to a DNA surface area of $a = 70$ Å^2. This energy is calculated by the numerical solution of the (1D) PB equation for an isolated charged cylinder in aqueous electrolyte solution. The results shown in Fig. 3 will later be used for calculating the lipoplex formation free energy and the phase diagram of the system.

Phase behavior

Consider an aqueous solution containing DNA strands of total length sD, N^+ cationic lipids, and N^0 neutral (helper) lipids; $N^+ + N^0 = N$. The total length of DNA associated in complexes will be denoted as sD_{C}, ($D_{\mathrm{C}} \le D$). Note that D_{C} is also the number of unit cells in the complex. The length distribution of the DNA strands is irrelevant, as both the naked DNA and the complex are treated as (immobile) macroscopic phases.

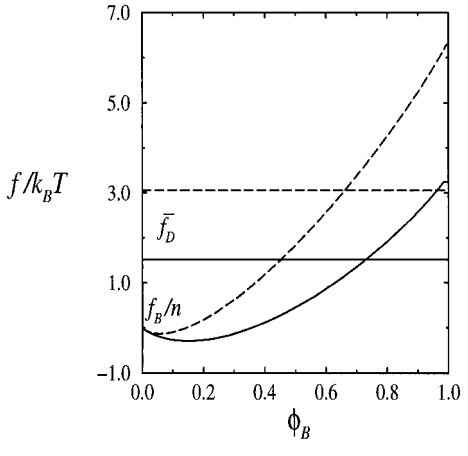

FIGURE 3 The free energy per molecule in the bare lipid bilayer (of area $a = 70$ Å^2 per molecule) as a function of the cationic lipid mole fraction. Also shown is the charging energy $\bar{f}_{\mathrm{D}} = af_{\mathrm{D}}/2\pi Rs$ of a naked DNA of surface area a. The solid and dashed curves correspond to $l_{\mathrm{D}} = 10$ Å and 50 Å, respectively.

As the concentration of monomeric lipids in solution is generally negligible, we can safely assume that all lipids are organized in bilayers which, in both the free and complexed states, are assumed to be planar. We find it convenient to express the total bilayer area, $A = Na$, in the form $A = sL$, so that L is the total "length" of the bilayer, if regarded as a strip of width s. We shall use $L_{\mathrm{C}} = \chi L$ and $L_{\mathrm{B}} = (1-\chi)L$ to denote the total length of the complexed and free bilayer, respectively. Note that $L_{\mathrm{C}} = dD_{\mathrm{C}}$, where d is the distance between DNA strands in the complex. Also, using N_{C}^+ to denote the number of cationic lipids in the complex, we define $L_{\mathrm{C}}^+ = (a/s)N_{\mathrm{C}}^+$. Similarly, we define $L_{\mathrm{B}}^+ = (a/s)N_{\mathrm{B}}^+$, $L_{\mathrm{C}}^0 = (a/s)N_{\mathrm{C}}^0$, $L_{\mathrm{B}}^0 = (a/s)N_{\mathrm{B}}^0$ and $L_{\mathrm{C}}^+ + L_{\mathrm{B}}^+ = L^+$, $L_{\mathrm{C}}^0 + L_{\mathrm{B}}^0 = L^0$. The mole fractions of cationic lipid in the complexed and free bilayer are given by $\phi_{\mathrm{C}} = N_{\mathrm{C}}^+/N_{\mathrm{C}} = L_{\mathrm{C}}^+/L_{\mathrm{C}}$ and $\phi_{\mathrm{B}} = N_{\mathrm{B}}^+/N_{\mathrm{B}}$, respectively. These two lipid compositions are generally different, but related to each other by the conservation condition ("lever rule")

$$\chi\phi_{\mathrm{C}} + (1-\chi)\phi_{\mathrm{B}} = m, \qquad (8)$$

where $m \equiv N^+/N = L^+/L$ is the overall mole fraction of cationic lipid in solution.

Finally, we introduce the (dimensionless) quantity

$$\rho = N_+/(sD/l) = (mL/D)(l/a), \qquad (9)$$

expressing the ratio between the total number of surface positive (lipid) charges and negative (DNA) charges in the system. Of particular interest is the "*isoelectric point*," $\rho = 1$. Experiment shows (at least for $m \approx 0.5$) that at this point all of the lipids and DNA in solution are involved in complex formation (Rädler et al., 1997). In the next section we shall show that this result holds for a wide range of lipid compositions m and, furthermore, that the isoelectric point corresponds to the minimum of the complex free energy f_{C}.

Experiment also shows that upon increasing the overall lipid-to-DNA ratio (L/D), at constant lipid composition (m), the system evolves through three distinct regions:

1. When L/D (equivalently, $\rho \propto L/D$) is small, the system is biphasic; the solution contains lipid-DNA complexes that coexist with excess, naked DNA. Thus, in this region, $D > D_{\mathrm{C}}$, whereas $L_{\mathrm{C}} = L$ (no free bilayer). The DNA-DNA distance in the complex is constant, $d = d_1(m)$, independent of ρ as long as $\rho \le \rho_1(m)$, which marks the onset of the next region. Once $\rho = \rho_1$, all of the DNA is complexed, so that $D_{\mathrm{C}} = D = L/d_1$, and hence, from Eq. 9, $\rho_1 = md_1(l/a)$. In general, $\rho_1 < 1$.
2. Between ρ_1 and a certain $\rho_2 = \rho_2(m) > 1$, the system is one-phasic: all of the DNA and lipid is involved in complex formation. Thus, $L_{\mathrm{C}} = L$, $D_{\mathrm{C}} = D$, and hence $d = L/D = (a/l)(\rho/m)$ increases linearly with the lipid/DNA ratio, from d_1 at ρ_1, through $d_{\mathrm{I}} = d_{\mathrm{I}}(m) = (a/l)/m$ at the isoelectric point ($\rho = 1$), to $d_2 = d_2(m)$ at $\rho_2(m) = md_2(l/a)$, which marks the onset of the third region. In general, $\rho_2 > 1$.

3. For large L/D ($\rho > \rho_2$) the system is again biphasic, containing complexes that coexist with an excess bilayer phase, $D_C = D$, $L_C < L$. In this region the system possesses an extra thermodynamic degree of freedom, namely, the lipid composition of the complex, ϕ_C (or, equivalently, ϕ_B, which is related to ϕ_C by Eq. 8). Thus, unlike in region 1, ϕ_C (hence ϕ_B) need not be equal to m. In other words, for any m and L/D, the system will adjust both d and ϕ_C so as to minimize its total free energy. Indeed, we shall see that in the excess bilayer region, both ϕ_C (hence ϕ_B) and d vary with ρ. It should be noted, however, that experimentally, $d \approx d_2(m)$ appears to be independent of ρ in region 3. This result will be discussed in more detail in the next section.

In principle, the system may also exhibit three-phase (complex/bilayer/DNA) coexistence as well as bilayer/DNA coexistence. However, these conditions correspond to very narrow regions of the phase diagram (low m values), where the complexes are either unstable or only marginally stable. We shall thus focus on the three-stage scenario outlined above.

Our analysis involves three possible phases: free DNA, free bilayer, and complex. The first two may be regarded as incompressible condensed phases. On the other hand, the complex is "compressible" because both the DNA-DNA spacing, d, and the interbilayer spacing, h, may vary with m and L/D. However, both experiment and our calculations (next section) show that in general, only d varies significantly with m and L/D, whereas h is essentially constant, $h \approx h^*$. In other words, for most ϕ_C and d, the complex free energy $f_C(\phi_C, d, h)$ has a narrow and deep minimum at h^*. Thus we can safely treat $f_C = f_C(\phi_C, d) = f_C(\phi_C, d, h = h^*)$ as a function of only two variables.

For given m and L/D (and given l_D), the number and nature of the phases in solution are determined by the minimum of the total free energy,

$$F = (D - D_C)f_D + D_C f_C(\phi_C, d) + (L - dD_C)\tilde{f}_B(\phi_B), \quad (10)$$

with respect to D_C, d, and ϕ_C (ϕ_B depends on these three variables through Eq. 8).

Setting $D_C = L/d$, $\phi_C = m$ in Eq. 10, and minimizing F with respect to d, we find the equilibrium condition for region 1,

$$f_C(m, d) - d\left(\frac{\partial f_C}{\partial d}\right)_m - f_D = \left(\frac{\partial (f_C/d)}{\partial (1/d)}\right)_m - f_D = 0. \quad (11)$$

This equation determines the equilibrium interaxis distance in the complex, $d = d_1(m)$, in the presence of excess free DNA. Based on this equation, we anticipate that d_1 will be smaller than the "optimal" value, $d^* = d^*(m)$, corresponding to the minimum of $f_C(m, d)$. This follows from the fact that the free energy of a DNA strand in a stable complex must be lower than in solution, and hence $f_D - f_C(m, d) > 0$, which means $(\partial f_C/\partial d)_{d=d_1} < 0$. Physically, the "overcrowding" ($d_1 < d^*$) of DNA strands in the complex results from the partial release of mobile counterions into solution upon bringing more DNA charges into contact with the cationic lipid charges. When $d = d_1$, this "overcharging" of the complex by DNA is balanced by DNA-DNA repulsion within the complex (the latter of which increases as d decreases).

In region 2, where all of the DNA and lipids are associated in complexes, $F = Df_C(m, d)$, and $d = L/D$ increases linearly with the lipid-to-DNA ratio. (The linear increase reflects our assumption that the bilayer is planar and laterally incompressible.) At some point within this region, generally very close to $\rho = 1$, the complex free energy is minimal (i.e., $d_1(m) \cong d^*(m)$). The uptake of bilayer into the complex continues beyond this point, as long as the added lipids enjoy lower free energy in the complex as compared to that in the free bilayer. Eventually, at some $d = d_2(m) > d^*$ (and $\rho = \rho_2(m) > 1$), interbilayer repulsion becomes sufficiently large to forbid further accommodation of bilayer in the complex, marking the onset of region 3. To support this qualitative description, let us first consider the hypothetical case of "blocked lipid exchange," where $\phi_B = \phi_C = m$. (This limit could perhaps be realized experimentally, as a transient state, if the rate of lipid exchange is small compared to that of complex formation.) Setting $D_C = D$, $\phi_C = \phi_B = m$ in Eq. 10, and minimizing F with respect to d, we find

$$\left(\frac{\partial f_C}{\partial d}\right)_m - \tilde{f}_B(m) = 0, \quad (12)$$

which determines $d_2 \equiv \hat{d}_2(m)$ for the case of blocked exchange. For this special case, let $\hat{\rho}_2(m)$ denote the value of ρ at the boundary between regions 2 and 3, corresponding to $\chi = dD/L = 1$ in Eq. 8. From Eq. 12 it follows that $d = \hat{d}_2(m)$ is constant throughout region 3 ($\rho > \hat{\rho}_2(m)$, or $1 > \chi > 0$). Because $\hat{d}_2(m)$ is also the maximum d in region 2, it follows that $\hat{\rho}_2(m) = m\hat{d}_2(l/a)$. Finally, because the bilayer charging energy, $\tilde{f}_B(m)$, is positive, it follows from Eq. 12 that $\hat{d}_2 > d^*$.

In the more general case of *free lipid exchange*, the values of d, ϕ_C, and ϕ_B in the bilayer-complex coexistence region are determined by the equilibrium conditions $(\partial F/\partial d) = 0$ and $(\partial F/\partial \phi_C) = 0$. Noting that in this region $D_C = D$ and $(dD/L)\phi_C + (1 - dD/L)\phi_B = m$ (see Eq. 8), we obtain

$$\left(\frac{\partial f_C}{\partial \phi_C}\right)_d = d\frac{d\tilde{f}_B}{d\phi_B} \quad (13)$$

$$\left(\frac{\partial f_C}{\partial d}\right)_{\phi_C} - \tilde{f}_B(\phi_B) = (\phi_C - \phi_B)\frac{d\tilde{f}_B}{d\phi_B}. \quad (14)$$

We could rewrite the last two equations in a slightly different form in terms of $\tilde{f}_C \equiv f_C/d$, the free energy per unit length of the complex, instead of f_C, the free energy per unit cell. Then, if d were constant ("incompressible complex"), Eqs. 13 and 14 would reduce to the familiar "common tangent construction" for $\tilde{f}_C$ and $\tilde{f}_B$, representing the coex-

istence conditions of two incompressible binary mixtures. If this were the case, we would also find that ϕ_C and ϕ_B are independent of χ. However, because the complexes are not incompressible, both d and ϕ_C (and hence also ϕ_B) may vary with χ, as will be shown in the next section.

RESULTS AND ANALYSIS

Following the discussion in the previous section, we shall first present and analyze the numerical results for the free energy and structure of an isolated DNA-lipid complex and then discuss the phase behavior of the solution. Comparison with detailed published data for L_α^c complexes is possible for only one kind of system: a solution containing an equimolar ($m = 0.5$) mixture of cationic (DOTAP) and nonionic helper (DOPC) lipids and linear (either λ-phage or plasmid) DNA, without added salt (Rädler et al., 1997). The bulk concentration of mobile ions in this system is low, but the exact concentration is unknown (as it is volume dependent). Thus, in most calculations, we have used $n_0 \approx 4 \times 10^{-3}$ M, corresponding to a Debye length $l_D = 50$ Å. Very similar properties and phase behavior of the complex were found for larger values of l_D. Partial results will also be presented for $l_D = 10$ Å, corresponding to physiological salt concentrations ($n_0 \approx 0.1$ M). In all of the calculations reported below, we have used $R = 10$ Å for the DNA radius and $a = 70$ Å^2 for the average area per (both cationic and neutral) lipid headgroup.

Complex structure and stability

The electrostatic (charging) free energy per unit cell of the complex, f_C, is shown as a function of d for several values of ϕ_C in Fig. 4 (for $s = 1$ Å, $l_D = 50$ Å). Similarly, Fig. 5 shows f_C as a function of ϕ_C for several values of d.

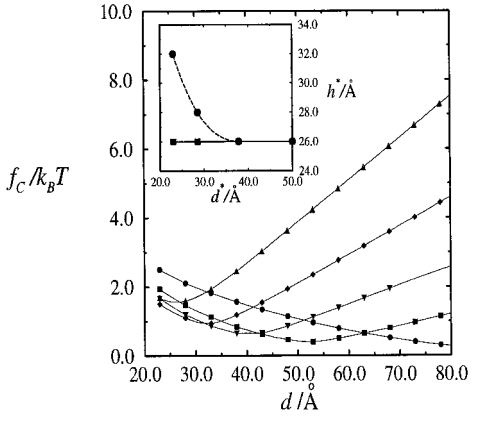

FIGURE 4 The free energy per unit cell of the complex as a function of the DNA-DNA spacing, for several different mole fractions of the cationic lipid: $\phi_C = 0.23$ (●), 0.39 (■), 0.50 (▼), 0.62 (◆), 0.78 (▲). The inset shows the optimal interbilayer distance, h^*, versus the optimal DNA-DNA spacing, d^*, for a low lipid composition, $\phi_C = 0.15$ (●). For all ϕ_C larger than ~0.2, h^* is constant (■).

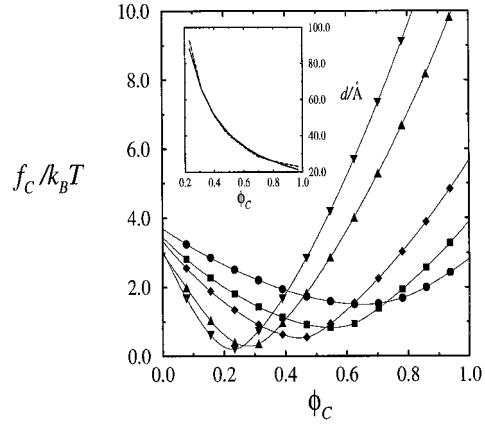

FIGURE 5 The free energy per unit cell of the complex, as a function of the lipid composition, for several values of the DNA-DNA spacing: $d = 23$ (●), 33 (■), 43 (◆), 73 (▲), 93 (▼) Å. The inset shows how the optimal spacing, d^* (——) and isoelectric spacing, d_I (——) vary with the lipid composition in the complex, revealing that d^* and d_I are essentially identical.

All of the results shown in Figs. 4 and 5 were obtained using $h = h^* = 26$ Å, corresponding to a minimal distance of 3 Å between the DNA and bilayer surfaces. This is the value of h^* observed experimentally for the L_α^c complex by Rädler et al. (1997). It should be noted, however, that h^* is larger than the minimal value of the interbilayer spacing, $h_{min} = 2R = 20$ Å. In fact, for most values of ϕ_C, our calculations show that the electrostatic free energy of the complex decreases monotonically as h decreases, including the region $h^* > h > h_{min}$. Thus we treat $h^* \approx 26$ Å as the effective range of a "hard-wall" potential, representing the short-range repulsive forces arising from hydration, protrusion, and other excluded volume interactions (Israelachvili, 1992; Israelachvili and Wennerström, 1990). Subject to this condition, we find that for all ϕ_C larger than ~0.2, the minimum in $f_C(\phi_C, d, h)$ is always at $h = h^*$, regardless of d. For very low values of ϕ_C (less than 0.2), we find, for low d's, that the optimal value of h increases as d decreases, as demonstrated for $\phi_C = 0.15$ in the inset to Fig. 4. Note, however, that for these low ϕ_C's, the minimum of f_C occurs at large d^*'s, where again, $h = h^*$. More generally, our conclusions regarding the complex structure and stability or the phase behavior of the system are not sensitive to small variations in h^*.

In Fig. 4 we see that the optimal DNA spacing in the complex, d^*, is a decreasing function of ϕ_C. Similarly, Fig. 5 shows that the optimal complex composition ϕ_C^* is a decreasing function of the DNA-DNA distance.

Qualitatively, these results are easily understood. The minima in the electrostatic free energy are expected to occur when the fixed negative charges on the DNA surface are balanced by the same number of positive charges on the bilayer surface, i.e., at the isoelectric point. At this point, the complex will remain electrically neutral, even if all of the mobile ions in its interior would be released into the bulk solution, thus increasing their translational entropy and con-

sequently lowering the free energy of the system. Of course, some counterions will always remain within the complex water gaps, as dictated by the bulk value of their chemical potentials. However, the concentrations of these mobile ions will be much smaller than in the diffuse layers near the surfaces of the noncomplexed DNA and membrane. Now the total charge on the bilayer surface is proportional to $d \times \phi$, whereas the total charge on the DNA surface is constant. Thus, at the isoelectric point $d_I(\phi_C) = (a/l)/\phi_C$, explaining the decrease in $d_I \cong d^*$ with ϕ_C. The inset to Fig. 5 shows how d_I and d^* vary with ϕ_C. The two curves are essentially identical, confirming that the complex free energy is, indeed, minimal at the isoelectric point. Thus, hereafter, we set $d_I \equiv d^*$.

Figs. 4 and 5 also reveal that the minimum value of the complex free energy $f_C^* \equiv f_C(\phi_C, d^*(\phi_C))$ varies rather weakly with ϕ_C. More generally, we note that as ϕ_C (or d) is changed, the complex can change its d (or ϕ_C), i.e., "cross" to a neighboring free energy curve, without significantly changing its free energy. This ability of the complex to change its composition (and d) at minimal free energy cost is manifested when complexes coexist with an excess bilayer phase, in which case ϕ_C and ϕ_B are determined by the minimum of F (rather than f_C), as will be demonstrated in the next section (Phase evolution).

Based on the numerical results for f_C, we can estimate the amplitude of interaxis fluctuations, $\Delta d = [\langle (d - d^*)^2 \rangle]^{1/2}$. Imagine that one DNA strand, say of length $\xi \cong 500$ Å, is displaced toward one of its neighbors by a distance δd, thus creating two unit cells of dimensions $d = d^* \pm \delta d$. Allowing the lipid composition in the new unit cells to relax (implying $\delta\phi = \phi(\delta d/d^*)$), the free energy cost of this fluctuation is $\delta f = \xi[f_C^*(d - \delta d) + f_C^*(d + \delta d) - 2f_C^*(d)] = \xi(\partial^2 f_C^*/\partial d^2)(\delta d)^2$. We find that $\delta f \approx 1\ k_B T$ for $\Delta d \cong |\delta d| \cong 1$ Å.

When $d < d^*$, there is a net negative surface charge on the complex "walls." To ensure electrical neutrality, positive mobile ions must be brought from the bulk solution into the confines of the complex, thus increasing the free energy of the system. As d decreases, the excess concentration of positive counterions increases, for two reasons: the increase in the excess surface charge and the decrease in the inner complex volume. The concomitant increase in the free energy of the complex, and hence the effective DNA-DNA repulsion, is due to the excess charging energy of the DNA surfaces, and the increased osmotic pressure of the counterions within the complex interior. (A simple electrostatic model accounting for this behavior will be described in the Discussion.)

Similarly, as d increases above d^*, negative mobile ions must be brought into the complex to balance the excess positive charge on the (lipid bilayer) surfaces. However, unlike in the $d < d^*$ region, where counterion confinement depends strongly on d, in this region counterion confinement is mainly due to the finite bilayer spacing h. Because h is constant, f_C is expected to increase *linearly* with d (in the large d region), as is indeed observed in Fig. 4. The rate of this increase, i.e., $\partial f_C/\partial d$, is proportional to the electrostatic free energy per unit area of the bilayer in the complex. This free energy is a sum of the bilayer charging energy, which increases with ϕ_C (see below) and the interbilayer repulsion energy. For most values of ϕ_C considered here, the complex conditions are those of the "Gouy-Chapman regime" (Andelman, 1995), where the interbilayer interaction energy is independent of the surface charge density. Thus the ϕ_C dependence of the asymptotic slope of f_C in Fig. 4 is mostly due to the charging energy of the lipid monolayers.

These notions are confirmed in Fig. 6, which shows the formation free energy of the complex, Δf_C, as a function of d for several values of ϕ_C. Note from Eq. 1 that this quantity, which represents the net stabilization energy of the complex, is obtained from f_C after subtracting the charging energy of the noncomplexed DNA and bilayer. Thus the steep variation of Δf_C at small values of d is dominated by the strong DNA-DNA repulsion (counterion confinement) in this regime. Similarly, the increase in Δf_C at high d's ($d \gg d^*$) is due almost exclusively to interbilayer repulsion. From the discussion above it follows that in this region $\partial \Delta f_C/\partial d$ should be nearly independent of ϕ_C, as confirmed by Fig. 6.

From the results in Fig. 6 we also conclude that stable complexes ($\Delta f_C < 0$) can be formed for a wide range of lipid compositions. The complex stabilization energies are on the order of a few $k_B T$'s per unit cell. For a "mesoscopic" complex, containing DNA strands of total length on the order of, say, 1 μm, this implies a total stabilization energy on the order of $10^4\ k_B T$.

In the previous section we emphasized the fact that the lateral distribution of the cationic lipid charges in the complex need not be uniform. Indeed, we find that the actual charge distribution is polarized, reflecting a compromise between the tendency to minimize the electrostatic energy on the one hand, and the unavoidable demixing entropy

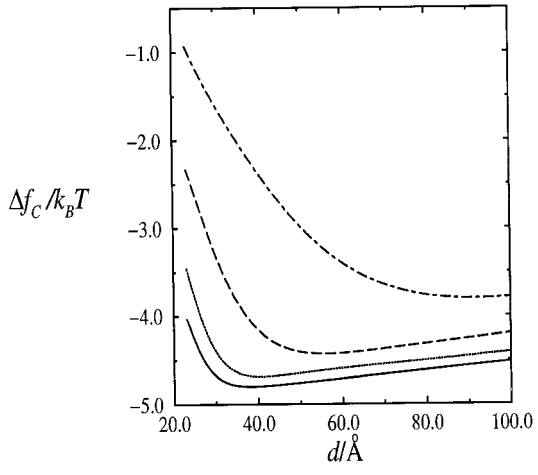

FIGURE 6 The formation free energy of the complex, as a function of d, for several values of the lipid composition, ϕ_C: 0.3 (– · – · –), 0.5 (——), 0.7 (· · · ·), 0.9 (——).

penalty on the other hand. The extent of spatial charge modulations in the complex is demonstrated in Fig. 7. The figure shows the variation in the local charge density $\eta(x)$ between two neighboring DNA strands, for complexes of three lipid compositions (high, low, and equimolar $\phi_C = \langle\eta(x)\rangle$), all at their isoelectric (i.e., optimal) value of d.

When ϕ_C is low, d^* is necessarily large. To effectively screen the negative DNA charges, cationic lipids must be displaced over a relatively large distance, resulting in a dramatic charge modulation. On the other hand, when ϕ_C is large, d is small, and the charge segregation is rather weak. In fact, in this case some of the charged lipids are shifted from the immediate vicinity of the DNA toward the center of the unit cell, as their optimal local concentration near the DNA strands is lower than ϕ_C. (Recall that the charge density on the DNA surface corresponds to one elementary charge per $\sim$110 Å^2. The average charge density on the bilayer surface is ϕ_C/a, which, for $\phi_C = 0.78$, corresponds to one elementary charge per $\sim$90 Å^2.) Intermediate though substantial charge modulation is found for the equimolar lipid mixture, $\phi_C = 0.5$. For this system we also show, for comparison, the charge density profile in the hypothetical case in which lipid segregation does not involve a demixing entropy penalty. (Namely, we artificially ignore the lipid mixing entropy contribution to f_C. The PB equation is then solved subject to the condition of constant electrical potential on the bilayer surfaces, as if they were conducting sheets.) As expected, the charge modulation in this system is still more dramatic than in the "real" complex.

Phase evolution

In Fig. 8, *A* and *B*, we show how d, the DNA-DNA spacing in the complex, varies with $\rho = m(l/a)L/D$, the (scaled) charged-lipid to DNA ratio in solution. The $d - \rho$ plots in Fig. 8 *a* were calculated for a solution of low salt content, $l_D = 50$ Å, and several different lipid compositions m. Similar calculations are shown in Fig. 8 *b* for $l_D = 10$ Å.

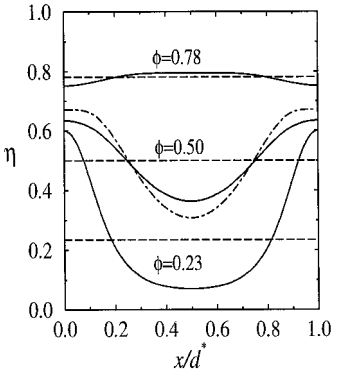

FIGURE 7 Spatial modulations of the cationic lipid charge within a unit cell of the complex. The local charge density profile, $\eta(x)$ (between two neighboring DNA strands), is shown (*solid lines*) for complexes of three lipid compositions: $\phi_C = 0.23$, 0.50, 0.78. All complexes are at their isoelectric value of d. The horizontal (*dashed*) lines correspond to uniform charge densities. The dash-dotted line, corresponding to $\phi_C = 0.5$, shows the charge density profile in a (hypothetical) complex in which charge modulation (lipid demixing) does not involve any entropy penalty. Note that in all but the highest ϕ_C case, cationic lipid is pushed out from between the DNA positions.

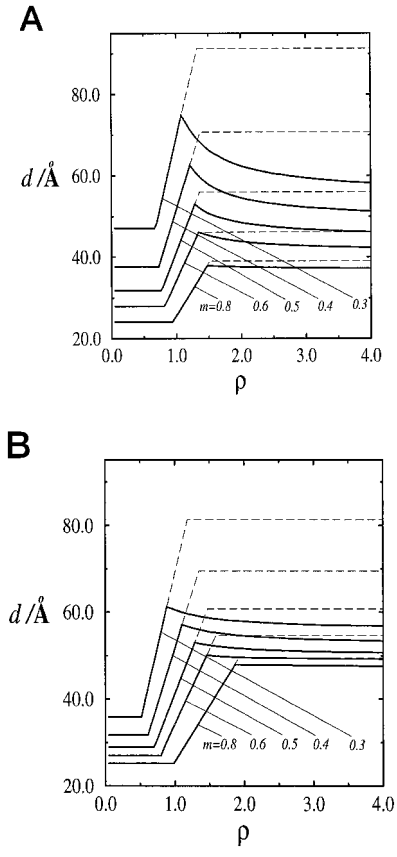

FIGURE 8 The DNA-DNA spacing d in the complex, as a function of the charged lipid-to-DNA ratio ρ, for several lipid compositions: $m = 0.3$, 0.4, 0.5, 0.6, 0.8 (*solid lines*). For each value of m, the dashed curve describes the variations in d for the case of blocked lipid exchange. (*A*) $l_D = 50$ Å. (*B*) $l_D = 10$ Å.

These calculations provide the most critical test of our model, because d is an experimentally measurable quantity. The experimental $d - \rho$ data points of Rädler et al. (1997), which were obtained for an equimolar lipid mixture ($m = 0.5$) and without added salt, are shown in Fig. 9. Also shown in this figure are the theoretical curves corresponding to $l_D = 10$ Å and 50 Å, both for $m = 0.5$. The low-salt ($l_D = 50$ Å) results show reasonable agreement with the experimental data. The inset to Fig. 9 shows how the (calculated) lipid compositions in the complex and free bilayer (in the "excess bilayer" regime) vary with the charged lipid-to-DNA ratio.

The $d - \rho$ "phase diagrams" in Figs. 8 and 9 were calculated using Eq. 11 for region 1 (excess DNA), and Eqs. 13 and 14 together with the lever rule (Eq. 8) for region 3 (excess bilayer). Equation 11 yields $d_1 = d_1(m)$ for the complex-DNA coexistence region 1, $0 \le \rho \le \rho_1(m) = md_1(l/a)$. In the one phase (complex) region 2, $d = L/D = (a/l)(\rho/m)$ varies linearly with ρ. The slope, $\partial d/\partial\rho$, in region

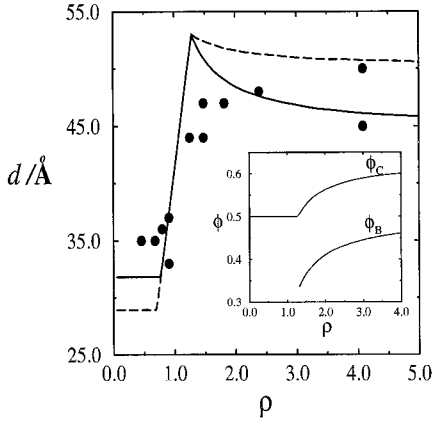

FIGURE 9 The DNA-DNA spacing, d, as a function of charged lipid-to-DNA ratio, ρ, for $m = 0.5$; $l_D = 50$ Å (*solid line*), 10 Å (*dashed line*). The dots are the experimental data of Rädler et al. (1997). The inset shows the variation in lipid composition in the complex and free bilayer as a function of the charged lipid-to-DNA ratio, for $l_D = 50$ Å.

2 is inversely proportional to the charged lipid mole fraction, m.

For region 3 the calculation is a little more complicated because of the additional lipid composition degree of freedom. For each value of m, the solution of Eqs. 13, 14, and 8 yield d, ϕ_C, ϕ_B as a function of ρ in the complex-bilayer coexistence region 3. The onset of this region is at $\rho_2 = md_2(m)(l/a)$. At this point all lipids are still complexed, and hence $\chi = d_2D/L = 1$ and $\phi_C = m$, but $\phi_B \neq m$; we generally find that at this point $\phi_B < m$, as demonstrated in Fig. 9 and in more detail in Fig. 10 below. As ρ increases (hence χ decreases) we find, for all values of m, that d decreases monotonically, reaching the asymptotic value $d = d_\infty(m)$ as $\rho \to \infty$. In this limit we have $\chi \to 0$ and hence $\phi_B \to m$, but now $\phi_C \neq m$; in general we find that, asymptotically, $\phi_C > m$. From Fig. 8 it is apparent that the change in d in region 3, i.e., the difference $d_2 - d_\infty$, is generally small, and is essentially negligible for low l_D and/or large m.

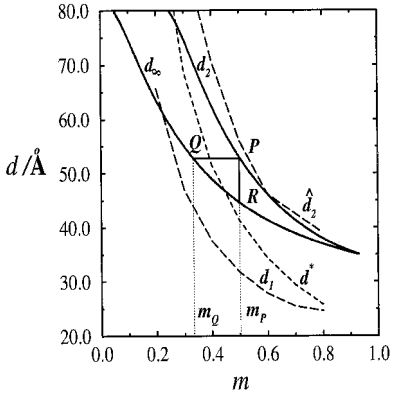

FIGURE 10 DNA-DNA distances in the complex at phase boundaries, as a function of the overall lipid composition in solution; d_2 and d_∞ represent, respectively, the interaxial distance at the onset of complex-bilayer coexistence and in the limit of infinite excess of bilayer. $\hat{d}_2$ marks the onset of complex-bilayer coexistence for the case of blocked lipid exchange. Also shown are the DNA-DNA spacing at the isoelectric point (d^*), and at the limit of the complex-DNA coexistence region (d_1) ($l_D = 50$Å).

The dashed curves in Fig. 8 show, for comparison, how d varies with ρ in the limit of "blocked lipid exchange." For this case, regardless of the value of m, we see that the onset of region 3 is postponed to a larger L/D ratio, corresponding to $\rho = \hat{\rho}_2 > \rho_2$ and consequently, $d = \hat{d}_2 > d_2$. For this special case $d = \hat{d}_2$ in region 3 is independent of ρ. The difference between the cases of "blocked" and "free" lipid exchange is particularly pronounced for small values of m.

Qualitatively, the difference $\hat{d}_2(m) - d_2(m) > 0$, which reflects the role of lipid exchange between the complex and the free bilayer, can be explained as follows. In the case of blocked exchange ($\phi_C = \phi_B = m$), a free bilayer first appears when the increase in f_C upon the addition of lipids to the complex becomes larger than the electrostatic free energy of these lipids when organized in a free bilayer (see Eq. 12). This happens at $\rho = \hat{\rho}_2(m)$ and $d = \hat{d}_2(m)$. Suppose now that, at this point, we allow for lipid exchange between the complex and the bilayer. The bilayer (charging) energy can be significantly reduced by diluting its charges with neutral lipids, which can be imported from the complex, thus making $\phi_B < m$. This, in turn, implies an increase in the complex charge density, from m to $\phi_C > m$. However, this change can be accommodated at a minimal free energy cost because, simultaneously, the complex can adjust (lower) its d to ensure better electrostatic balance. The net result of this lipid-demixing process is an increase in the amount of free bilayer. Although imaginary, this process clearly accounts for the "earlier" appearance ($\rho_2 < \hat{\rho}_2$, $d_2(m) < \hat{d}_2(m)$) of bare bilayer in a system where lipid exchange is free.

In Fig. 10 we show how d_2 and d_∞, the values of d at the boundaries of region 3, $\chi = 1$ and $\chi = 0$, respectively, vary with the overall lipid composition m. The figure also shows $d_1(m)$, the value of the interaxis distance in the complex, at the phase boundary between regions 1 and 2. Two additional curves, marked $d^*(m)$ and $\hat{d}_2(m)$, describe the interaxis distance at the isoelectric point and the boundary between regions 2 and 3, respectively, for the case of blocked lipid exchange.

The d_2 and d_∞ curves in Fig. 10 can be viewed as a "distillation diagram," prescribing the lipid compositions in complexes (of well-defined d) and free bilayers, when these two phases coexist in solution. More explicitly, consider a pair of points, such as P and Q, one on the d_2 and the other on the d_∞ curve, both corresponding to the same value of d. Then the projections of these points on the m axis, $\phi_C = m_P$ and $\phi_B = m_Q$, give the lipid compositions of the complex and free bilayer, for all values of m in the range $\phi_C \geq m \geq \phi_B$, provided the interaxis distance in the complex is d. This follows from the fact that, for this d, the points ϕ_B and ϕ_C represent the unique solution of the coexistence conditions (Eqs. 13 and 14). The relative amounts of lipid in the complex and the bilayer are dictated by the "lever rule," $\chi\phi_C + (1 - \chi)\phi_B = m$. In particular, when $\chi = 1$ and hence

$\phi_C = m$ (and $d = d_2$, point P), ϕ_B is the bilayer composition at the onset of region 3; similarly, when $\chi = 0$ and hence $\phi_B = m$ ($d = d_\infty$, point Q), ϕ_C is the asymptotic value of the complex composition. Experimentally it is of course easier to follow a vertical line, m = constant, such as that between points P and R. Any point on this line dictates a given value of d and hence, as above, a pair of coexisting compositions ϕ_C, ϕ_B. Because m is known, one obtains χ using the lever rule, and then the lipid/DNA ratio from $\rho = d(m/\chi)(l/a)$.

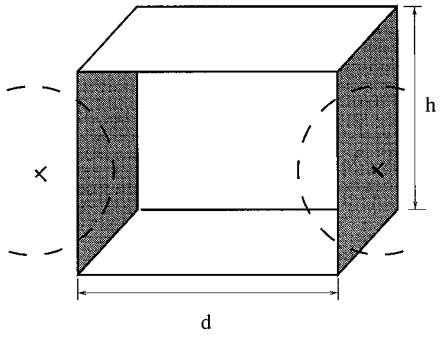

FIGURE 11 The complex unit cell used in the box model. The broken circles illustrate the DNA cross section. In the model these are the shaded surfaces.

DISCUSSION AND SUMMARY

We have seen in the above that interbilayer repulsion in the complex is responsible for the fact that the amount of bilayer that the complex can accommodate is finite, resulting in the appearance of a free bilayer phase once ρ exceeds $\rho_2(m) > 1$. Similarly, inter-DNA repulsion is responsible for the finite amount of DNA (in excess of that at the isoelectric point) that can be incorporated into the complex, resulting in the appearance of free DNA in solution when ρ falls below $\rho_1(m) < 1$. In the previous section, based on numerical calculations of the complex free energy and the coexistence conditions, we have shown how $\rho_1(m)$, $d_1(m) = \rho_1(m)(a/lm)$, $\rho_2(m)$ and $d_2(m) = \rho_2(m)(a/lm)$ vary with m. Now we provide a qualitative interpretation of these results, based on a simple "box" model of the complex. As we shall see, this model, although highly approximate, captures the essential physical principles governing the complex stability, and yields simple closed-form expressions for d_1, d_2, ρ_1, and ρ_2.

A simple box model

The complex unit cell may be viewed as a box, bounded ("above and below") by two positively charged lipid bilayer "walls" and (to the "left and right") by two negatively charged DNA "walls." The third dimension of this box, along the DNA axis direction, is infinite. The free energy of the complex reflects the charging energy of these walls, as well as the interactions between these charged surfaces (associated with the confinement of mobile ions to the complex "box"). Similar factors would dictate the complex free energy if the DNA surfaces were planar rather than curved, as shown in Fig. 11, which illustrates our box model. Of course, the finite curvature of real DNA surfaces is important for determining the numerical value of the complex free energy, but not the qualitative dependence of this quantity on such factors as the lipid charge density (m) and the asymmetry (d/h ratio) of the unit cell. Thus our first approximation is to replace the curved DNA surfaces with planar surfaces of height h, extending between the two planar bilayers. The distance between these walls will be denoted as d. (As indicated in Fig. 11, this d represents an intermediate value, smaller than the interaxis separation and larger than the intersurface spacing between neighboring DNA rods. An exact identification of d is irrelevant, as all of our conclusions involve the ratio d/d^*.)

The complex free energy is minimal at the isoelectric point where the net charge on the complex walls is zero. Above the isoelectric point ($\rho > 1$, $d > d^*$) the net charge on the complex walls is positive, with the excess, uncompensated charge spread over the bilayer surfaces. Similarly, when $\rho < 1$, an excess negative charge is spread over the DNA surfaces. The complex free energy will be calculated based on two assumptions reflecting these notions. First, it will be assumed that the electrostatic free energy of the complex arises completely from the excess charging of the bilayer surfaces when $\rho > 1$ and from the excess charge on the DNA surfaces when $\rho < 1$. Second, to model the free energy between a pair of charged (e.g., bilayer) walls, we shall treat them as infinite two-dimensional surfaces, in the region where the Debye length (l_D) greatly exceeds the Gouy-Chapman length (l_C). (More specifically, we shall consider the "Gouy-Chapman regime," where l_D is larger than l_C, as well as the spacing between the charged surfaces, i.e., d and h).

For $\rho > 1$, the net charge density on the bilayer surfaces is $\sigma^+_{net} = (d\sigma^+ - h\sigma^-)/d = \sigma^+ - (h/d)\sigma^-$, where $\sigma^+ = em/a$ is the actual cationic surface charge density. Similarly, $\sigma^- = e/2hl$ is the charge density on the planar surface representing (one-half of) the DNA envelope. In analogy to the bilayer composition, we define $\bar{m} = (a/e)\sigma^- = a/2hl$ as the dimensionless charge density ("composition") of the DNA surface. (Recall that $l = 1.7$ Å is the separation between charges along a DNA strand. Using also $a = 70$ Å^2 and $h = 26$ Å, we find $\bar{m} \approx 0.8$.) The excess charge density on the bilayer surfaces is given by

$$\phi = m - \frac{h}{d}\bar{m} = m\left(1 - \frac{d^*}{d}\right) \qquad (\rho > 1). \qquad (15)$$

Similarly, the excess charge density on the DNA surfaces is given by

$$\bar{\phi} = \bar{m} - \frac{d}{h}m = \bar{m}\left(1 - \frac{d}{d^*}\right) \qquad (\rho < 1). \qquad (16)$$

For the electrostatic free energy of the complex, above the isoelectric point, we write

$$f_C = Ad(2\phi[\ln(D\phi) - 1] + B/h) \qquad (\rho > 1), \quad (17)$$

whereas below the isoelectric point,

$$f_C = Ah(2\bar{\phi}[\ln(D\bar{\phi}) - 1] + B/d) \qquad (\rho < 1), \quad (18)$$

where $A = 2sk_BT/a$, $D = 4\pi l_B/\kappa a$, and $B = \pi a/2l_B$ are constants; s denotes the (arbitrary) depth of the unit cell. The first term in Eq. 17 accounts for the excess charging energy of the bilayer surfaces (from 0 to ϕ) in the low salt (high l_D) limit, and follows from Eq. 7 for $p \approx q \gg 1$. The second term in this equation represents the electrostatic interaction between two equally charged surfaces, separated by a distance h, corresponding to the conditions defining the Gouy-Chapman region ($h \gg (1/p\kappa) \equiv l_C$). Equation 18 is, similarly, the electrostatic energy corresponding to excess (negative) charge on the DNA surfaces, whose area is proportional to h and whose separation is d.

To solve the coexistence conditions, we also need the free energies of the bare bilayer and the naked DNA. The electrostatic free energy of the bilayer is given by the first term in Eq. 17, with the actual charge, m, replacing the net charge ϕ; namely, $f_B = Ad(2m[\ln(Dm) - 1])$. Our analysis of the bilayer-complex coexistence will be limited to the simpler case of "blocked lipid exchange." In this case the lipid mixing free energy in the free bilayer and the complex are identical and can thus be disregarded. For the charging energy of the naked DNA surfaces (which, for consistency, we treat as planar), we have $f_D = Ah(2\bar{m}[\ln(D\bar{m}) - 1]$.

Using the above expressions for f_C and f_B in the bilayer-complex coexistence condition (Eq. 12), we obtain

$$\ln\left(1 - \frac{d}{d^*}\right) + \frac{d^*}{d} + \frac{B}{2hm} = 0 \qquad (\rho > 1). \quad (19)$$

The solution of this equation, $d = \hat{d}_2(m)$, determines the value of d at the boundary between regions 2 and 3 for the case of blocked lipid exchange. Correspondingly, $\hat{\rho}_2(m) = m\hat{d}_2(m)(l/a)$.

Suppose first that $B = 0$, as would be the case if there were no repulsion between the charged bilayer surfaces in the complex. For this hypothetical case we find that $\hat{d}_2(m) \to \infty$. This result is consistent with the fact that, for all finite d, the effective charge on the complexed bilayer, ϕ, is smaller than that of the free bilayer, m. Consequently, in the absence of interbilayer repulsion, the complex free energy is always lower than that of the free bilayer, which explains the unbound uptake of bilayer into the complex. We know, however, that $\hat{d}_2(m)$ is not much larger than d^* (see Fig. 8); i.e., bilayer repulsion is important. For $d^*/d \lesssim 1$, we find from Eq. 19 that

$$\hat{d}_2 = d^*/(1 - \exp[-(1 + B/2hm)]) \qquad (\rho > 1), \quad (20)$$

indicating that $\hat{d}_2(m)/d^*$ is a decreasing function of m. For the molecular parameters used in our calculations, we find that $B/h \approx 0.6$. For $m = 0.5$, this implies $\hat{d}_2/d^* \approx 1.25$, in surprisingly good agreement with the value obtained from our detailed calculations, $\hat{d}_2/d^* \approx 1.3$.

Using the complex-DNA coexistence condition (Eq. 11), an equation similar to Eq. 19 can be derived for $d/d^* = d_1(m)/d^*$ in the region $\rho < 1$. Here, for $d/d^* \lesssim 1$, we find

$$d_1 = d^*(1 - \exp[-(1 + Bm/h\bar{m}^2)]) \qquad (\rho < 1). \quad (21)$$

From this equation it follows that as m increases, $d_1 \to d^*$, in qualitative agreement with the results shown in Fig. 8. For the equimolar system ($m = 0.5$), we find $d_1/d^* \approx 0.77$, which, perhaps fortuitously, is nearly identical to the result derived from our detailed calculations.

Considering the drastic approximations and assumptions involved in the formulation and solution of the simple box model, we obviously do not expect this model to confirm all of our findings. For instance, we did not even try to include in this model the (important) effects of lipid charge modulations, or to account for the more complicated case of free lipid exchange. Note also that none of the above equations reflect the dependence of the phase boundaries on the salt concentration in the system (which follows from the fact that the model was applied for the Gouy-Chapman region, corresponding to low salt solutions). Nevertheless, as stated earlier, the simple box model does capture the basic features of the complex-DNA and complex-bilayer coexistence.

Other models

Bruinsma (1998) has independently discussed how the nonlinear Poisson-Boltzmann theory can account qualitatively for the features observed by Rädler et al. (1997) for the structural evolution of DNA-cationic lipid complexes as a function of charged lipid-to-DNA ratio. Because he develops an analytical (rather than numerical) solution of the problem, he is constrained to introducing several simplifications (e.g., low surface charge densities, and no added salt) in addition to those discussed in our present work. Nevertheless, his model of the lipoplex is consistent with ours and provides a slightly different flavor to its interpretation. He too allows for spatial variation of the bilayer surface charge density, induced by interaction with the oppositely charged DNA strands, and, while not solving explicitly for $\eta(x)$, is careful to treat self-consistently the corresponding boundary condition for the electrostatic potential at this surface. Also in his treatment, two-phase coexistence between the L_α^c complex and excess DNA (low ρ) and excess lipid (high ρ) are identified by chemical potential relations equivalent to our Eqs. 11–14. However, unlike in our model, where the naked DNA is treated as a macroscopic phase (embedded in a dilute aqueous salt solution), Bruinsma's expression for the free energy of DNA in solution is based on a cell-like model for the pure counterion case (Lifson and Katchalsky, 1954), which involves a $\ln \Phi$ term, with Φ denoting the volume fraction of the free DNA. This Φ dependence then enters the DNA-lipoplex

equilibrium condition, implying a weak dependence of d on ρ at finite Φ (excess DNA, our region 1). Around $\Phi = 0$, which is identified as the isoelectric point, d shows a singular dependence on Φ (equivalently, ρ), increasing steeply from a low value to a higher one, the latter determined by lipoplex-bilayer coexistence. In other words, the isoelectric point is unstable with respect to uptake of either DNA or bilayer. In our terminology this picture implies a sudden jump from d_1 to d_2, and $\rho_1 \equiv \rho^* \equiv \rho_2$, i.e., no one-phase (complex) region. This result is at variance with our findings. On the other hand, Bruinsma's conclusions regarding region 3 (excess bilayer) are similar to ours. He explains the constancy of DNA-DNA spacing at high ρ values in terms of the repulsive interaction between bilayers within the complex; this repulsion increases with the deviation from the isoelectric point and hence ultimately overwhelms the effect of counterion release that had been driving uptake of the lipid bilayer. Recall that we had explained the uptake of DNA ($\rho < 1$) and bilayer ($\rho > 1$) in terms of the entropy gain of bound counterions (relative to their state in "free" DNA or "free" bilayer, respectively) as they move into the complex with significantly lower concentrations. See, for example, the excess charge densities defined by Eqs. 15 and 16 in the "box" model, each of which is generally quite small compared to their "bare" values in the free macroions (DNA or liposome). This phenomenon appears still more dramatically in the approximate analytical work of Bruinsma leading to "isoelectric instability."

Dan (1997) has proposed a quite different explanation of the constancy of DNA spacings at low and high values of charge lipid to DNA. Her argument is based on the idea that elastic deformation of the bilayer by its interaction with DNA gives rise to an effective attraction between the DNA strands. At high ρ values (i.e., low DNA content relative to lipid, at fixed neutral-to-cationic lipid ratio; note that Dan's ratio ρ is defined in a way that makes it inversely proportional to ours), all of the DNA in solution is intercalated in the sandwich complexes, which in turn coexist with excess liposomes. Here the DNA spacing takes on its optimum value, d_o, reflecting directly the competition between these relatively long-range attractions (taken to vary linearly with d) and the exponentially screened, electrostatic repulsions. Upon decreasing ρ and adding DNA, more and more of the "free" bilayer is bound, with the DNA spacing remaining constant at d_0. This region persists down to ρ values that are low enough that there is no longer any "free"/"excess" bilayer. A further decrease in ρ leads to a decrease in d spacing, because the strand-bilayer adsorption energy overwhelms the strand-strand repulsion. But, according to Dan, this drop in d is arrested by the onset of the isoelectric point, beyond which, she argues, the DNA spacing will remain constant at a value equal to the average distance d_a between cationic lipid charges (or to the hard-core diameter of the DNA strands, if this quantity is larger than d_a). This scenario, then, is significantly different from the present one and Bruinsma's, not only because of the central role ascribed to an effective attraction between intercalated DNAs, but also because it underplays the special nature of the isoelectric complex as one that tends to suck in both excess DNA and cationic lipid bilayers because of the lower concentrations made available to bound counterions than in the "free" DNA and "free" liposomes.

CONCLUDING REMARKS

Using an electrostatic model for the lipoplex and straightforward, though appropriately modified, thermodynamic expressions for phase equilibria, we were able to explain the structure and phase evolution in aqueous solutions containing DNA, neutral-cationic liposomes, and L_α^c lipoplexes. Our treatment of these phenomena was based on the premise that the lipid bilayers in the complex are perfectly planar and of constant thickness, for all lipid compositions. This, of course, is an approximation, valid for lipid bilayers of high bending rigidity and small spontaneous curvature, consisting of lipids with similar chain lengths. On the other hand, as mentioned in the Introduction, there is strong experimental evidence for the existence of nonlamellar lipoplexes, in particular, "honeycomb" (or H_{II}^c) complexes whose symmetry is that of the inverted hexagonal (H_{II}) lipid phase. In fact, it is not hard to imagine that this would be the preferred complex geometry for a lipid mixture whose (monolayer's) spontaneous curvature is negative (e.g., DOPE-containing mixture).

Quite generally, variations in the lipid composition imply variations in both the bending rigidity and the spontaneous curvature of the monolayers constituting a lipid membrane. In an L_α^c complex, for instance, softening the membrane would most probably involve curvature modulations of the lipid bilayers around the DNA strands. Correlated curvature modulations between stacked (lipoplex) bilayers may result in 3D order ("locking") of the DNA strands in the complex. If, by compositional variations, the lipid membranes change both their rigidity and spontaneous curvature, a structural phase transition may take place between one complex geometry and another (e.g., $L_\alpha^c \rightarrow H_{II}^c$). This scenario is corroborated by very recent experiments (Safinya, unpublished observations). Theoretical work along these lines is in progress.

APPENDIX: THE NUMERICAL PROCEDURE

In solving the full nonlinear Poisson-Boltzmann equation, we follow previous calculations of the electrostatic potential, which employed Newton-Raphson iterations of the Laplacian (Carnie et al., 1994; Stankovich and Carnie, 1996). The problem is thus reduced to a sequence of linear elliptic equations of the form

$$\nabla^2\psi_{n+1} - (\cos\psi_n)\psi_{n+1} = \sinh\psi_n - (\cosh\psi_n)\psi_n, \qquad (22)$$

in which ψ_n is the electrostatic potential in the nth iteration step. (The value of the initial guess, ψ_0, can be chosen arbitrarily, and was in general set to $\psi_0 = 0$ in our calculations.) As $n \rightarrow \infty$, ψ_n converges to the solution of the full nonlinear equation. In practice, fewer than 50 iterations ensures $|\psi_n - \psi_{n+1}| < 10^{-3}$ for all grid points.

The linear elliptic problem was solved in each iteration by using the publicly available GENCOL routine (Houstis et al., 1985). This procedure can solve the linear equation on an arbitrary (closed) domain, using collocation with bicubic Hermite functions. In most cases, a 40×40 evenly spaced grid was used, but sometimes a variably spaced grid was also used.

For the lipid membrane, a nonlinear boundary condition (see Eq. 5) must be solved, stating the relation between the surface charge density, the potential ψ, and the Lagrange multiplier $\lambda(\psi)$. This can be handled through the use of a second Newton-Raphson iteration on the boundary condition, in addition to the one on the Laplacian. The two iterations can then proceed simultaneously. Writing Eq. 5 in the form

$$\frac{\partial \psi}{\partial y} = g(\psi) = \frac{\frac{1}{\alpha} e^{-(\psi+\lambda)}}{(1-\phi)/\phi + e^{-(\psi+\lambda)}}, \tag{23}$$

the Newton-Raphson iteration for the boundary condition would result in

$$\frac{\partial \psi_{n+1}}{\partial y} - \psi_{n+1} g'(\psi_n) = g(\psi_n) - \psi_n g'(\psi_n). \tag{24}$$

For $g'(\psi)$ we chose a "modified" derivative:

$$g'(\psi) = -\frac{\frac{1}{\alpha}\frac{1-\phi}{\phi} e^{-(\psi+\lambda)}}{\left[\frac{1-\phi}{\phi} + e^{-(\psi+\lambda)}\right]^2}. \tag{25}$$

In each iteration step the potential calculated in the previous step is used to evaluate λ, using Eq. 3. This value of λ is used to determine the boundary condition for the lipid bilayer through Eq. 24. It is then possible to solve Eq. 22 for the current step, etc.

Once the potential is found, it now remains to evaluate the free energy of the complex due to the charging and mixing processes. In principle, f_C could be evaluated by using Eq. 2. For numerical purposes it is more convenient to use the equivalent form:

$$\begin{aligned}\frac{f_C}{kT} = {} & \frac{1}{2}\int_{S_{III}} \frac{\sigma^-}{e}\psi \, dS + \frac{1}{2a}\int_{S_V} \eta\psi \, dS \\ & + \frac{\kappa^2}{4\pi l_B}\int_v \left(\frac{1}{2}\psi \sinh\psi - \cosh\psi + 1\right) dv \\ & + \frac{1}{a}\int_{S_V}\left[\eta \ln\frac{\eta}{\phi} + (1-\eta)\ln\frac{1-\eta}{1-\phi}\right] dS \\ & + n[\phi \ln\phi + (1-\phi)\ln(1-\phi)],\end{aligned} \tag{26}$$

where $n = N_C/D_C$ is the number of lipid molecules in the unit cell. (The passage from Eq. 2 to Eq. 26 involves using 1) the identity $(\nabla\psi)^2 = \nabla(\psi\nabla\psi) - \psi\nabla^2\psi$, 2) the Gauss theorem to convert the volume integral of $\nabla(\psi\nabla\psi)$ to a surface integral over $\psi\nabla\psi \propto -\psi\eta$, 3) the use of the PB equation (Eq. 4) for $\nabla^2\psi$ and the Boltzmann distributions: $n_\pm = n_0 \exp(\mp\psi)$.) This procedure precludes the need for using the derivatives of the potential (which are prone to a larger numerical error).

We thank Cyrus Safinya for several helpful discussions and information concerning his unpublished experiments. We also thank Joachim Rädler, Tim Salditt, Ilya Koltover, Brigitta Sternberg, and Chezy Barenholtz for helpful comments, and Robijn Bruinsma and Nily Dan for reprints of their work.

The financial support of the Israel Science Foundation (AB-S grant 8003/97), the U.S.-Israel Binational Science Foundation (AB-S and WMG, grant 94/130), and the National Science Foundation (WMG, grant NSF-DMR-9708646) is gratefully acknowledged. SM thanks the Minerva Stiftung for a postdoctoral fellowship. The Fritz Haber research center is supported by the Minerva Foundation, Munich, Germany.

REFERENCES

Andelman, D. 1995. Electrostatic properties of membranes: the Poisson-Boltzmann theory. pages 603–642 of: Lipowsky, R., and Sackmann, E. (eds), Structure and Dynamics of Membranes, second edn., vol. 1. Amsterdam: Elsevier,

Bruinsma, R. 1998. Electrostatics of DNA-cationic lipid complexes: isoelectric instability. *Eur. Phys. J.* (in press).

Carnie, S. L., D. Y. C. Chan, and J. Stankovich. 1994. Computation of forces between spherical colloidal particles: nonlinear Poisson-Boltzmann theory. *J. Colloid Interface Sci.* 165:116–128.

Dan, N. 1996. Formation of ordered domains in membrane-bound DNA. *Biophys. J.* 71:1267–1272.

Dan, N. 1997. Multilamellar structures of DNA complexes with cationic liposomes. *Biophys. J.* 73:1842–1846.

Dan, N. 1998. The structure of DNA complexes with cationic liposomes—cylindrical or lamellar? *Biophys. Biochim. Acta.* 1369:34–38.

Felgner, P. L., T. R. Gadek, M. Holm, R. Roman, H. W. Chan, M. Wenz, J. P. Northrop, G. M. Ringold, and M. Danielsen. 1987. Lipofectin: a highly efficient, lipid-mediated DNA transfection procedure. *Proc. Natl. Acad. Sci. USA.* 84:7413–7417.

Felgner, P. L., and G. M. Ringold. 1989. Cationic liposome mediated transfection. *Nature.* 331:461–462.

Felgner, P. L., Y. J. Tsai, and J. H. Felgner. 1996. Advances in the design and application of cytofectin formulations. *In* Handbook of Nonmedical Applications of Liposomes. D. D. Lasic and Y. Barenholz, editors. CRC Press, Boca Raton, Florida. 43–56.

Gershon, H., R. Ghirlando, S. B. Guttman, and A. Minsky. 1993. Mode of formation and structural features of DNA-cationic liposome complexes used for transfection. *Biochemistry.* 32:7143–7151.

Gustafsson, J., G. Arvidson, G. Karlsson, and M. Almgren. 1995. Complexes between cationic liposomes and DNA visualized by cryo-TEM. *Biophys. Biochim. Acta.* 1235:305–312.

Helfrich, W. 1973. Elastic properties of lipid bilayers: theory and possible experiments. *Z. Naturforsch.* 28:693–703.

Honig, B., and A. Nicholls. 1995. Classical electrostatics in biology and chemistry. *Science.* 268:1144–1149.

Houstis, E. N., W. F. Mitchell, and J. R. Rice. 1985. Collocation software for second order elliptic partial differential equations. *ACM Trans. Math. Software.* 11:379–418.

Hui, S. W., M. Langner, Y-L. Zhao, R. Patrick, E. Hurley, and K. Chan. 1996. The role of helper lipids in cationic liposome-mediated gene transfer. *Biophys. J.* 71:590–599.

Israelachvili, J. N. 1992. Intermolecular and Surface Forces, 2nd Ed. Academic Press, San Diego.

Israelachvili, J. N., and H. Wennerström. 1990. Hydration or steric forces between amphiphilic surfaces? *Langmuir.* 6:873–876.

Lasic, D. D., H. Strey, M. C. A. Stuart, R. Podgornik, and P. M. Frederik. 1997. The structure of DNA-liposome complexes. *J. Am. Chem. Soc.* 119:832–833.

Lekkerkerker, H. N. W. 1989. Contribution of the electric double layer to the curvature elasticity of charged amphiphilic monolayers. *Physica A.* 159:319–328.

Lifson, S., and A. Katchalsky. 1954. The electrostatic free energy of polyelectrolyte solutions. II. Fully stretched macromolecules. *J. Polym. Sci.* 13:43–55.

May, S., and A. Ben-Shaul. 1997. DNA-lipid complexes: stability of honeycomb-like and spaghetti-like structures. *Biophys. J.* 73: 2427–2440.

Mok, K. W. C., and P. R. Cullis. 1997. Structural and fusogenic properties of cationic liposomes in the presence of plasmid DNA. *Biophys. J.* 73:2534–2545.

Podgornik, R., D. Rau, and V. A. Parsegian. 1989. The action of interhelical forces on the organization of DNA double helices: fluctuation-enhanced decay of electrostatic double layer and hydration forces. *Macromolecules.* 22:1780–1786.

Podgornik, R., D. Rau, and V. A. Parsegian. 1994. Parameterization of direct and soft steric-undulatory forces between DNA double helical polyelectrolytes in solution of several different anions and cations. *Biophys. J.* 66:962–971.

Rädler, J. O., I. Koltover, T. Salditt, and C. R. Safinya. 1997. Structure of DNA-cationic liposome complexes: DNA intercalation in multilamellar membranes in distinct interhelical packing regimes. *Science.* 275: 810–814.

Salditt, T., I. Koltover, J. O. Rädler, and C. R. Safinya. 1997. Two dimensional smectic ordering of linear DNA chains in self-assembled DNA-cationic liposome mixtures. *Phys. Rev. Lett.* 79:2582–2585.

Stankovich, J., and S. L. Carnie. 1996. Electrical double layer interaction between dissimilar spherical colloidal particles and between a sphere and a plate: nonlinear Poisson-Boltzmann theory. *Langmuir.* 12: 1453–1461.

Sternberg, B. 1996. Morphology of cationic liposome/DNA complexes in relation to their chemical composition. *J. Liposome Res.* 6:515–533.

Sternberg, B., F. L. Sorgi, and L. Huang. 1994. New structures in complex formation between DNA and cationic liposomes visualized by freeze-fracture electron microscopy. *FEBS Lett.* 356:361–366.

Strey, H. H., V. A. Parsegian, and R. Podgornik. 1997. Equation of state for DNA liquid crystals: fluctuation enhanced electrostatic double layer repulsion. *Phys. Rev. Lett.* 78:895–898.

Tarahovsky, Y. S., R. S. Khusainova, A. V. Gorelov, T. I. Nicolaeva, A. A. Deev, A. K. Dawson, and G. R. Ivanitsky. 1996. DNA initiates polymorphic structural transitions in lecithin. *FEBS Lett.* 390:133–136.

Verwey, E. J. W., and J. Th. G. Overbeek. 1948. Theory of the Stability of Lyophobic Colloids. Elsevier, New York.

Wagner, K., E. Keyes, T. W. Kephart, and G. Edwards. 1997. Analytical Debye-Hückel model for electrostatic potentials around dissolved DNA. *Biophys. J.* 73:21–30.

Zuidam, N. J., and Y. Barenholz. 1997. Electrostatic parameters of cationic liposomes commonly used for gene delivery as determined by 4-heptadecyl-7-hydroxycoumarin. *Biophys. Biochim. Acta.* 1329:211–222.